

# Quantum interference of multimode two-photon pairs with a Michelson interferometer

Fu-Yuan Wang, Bao-Sen Shi,<sup>\*</sup> and Guang-Can Guo

*Key Laboratory of Quantum Information,*

*University of Science and Technology of China, Hefei 230026, China*

(Dated: October 29, 2018)

## Abstract

We experimentally observe the two-photon interference of multimode photon pairs produced by an optical parametric oscillator far below threshold via a michelson interferometer, which shows a multi-peaked structure. We find that the correlation function when the interferometer is unbalanced is clearly dependent on the path difference and phase between two interfering beams, but the shape of correlation function in balanced case is independent on the small path difference and phase beside the height. All experimental results are well agreed with the theoretical prediction.

PACS numbers: 42.50.St, 42.50.Ar, 42.65.Lm

arXiv:0806.4260v1 [quant-ph] 26 Jun 2008

---

<sup>\*</sup>Electronic address: drshi@ustc.edu.cn

Entangled photon pair source, as an essential tool, plays an important role in quantum information processing and quantum optics field[1, 2, 3, 4, 5]. By far, the common way to generate an entangled photon pair is the process of spontaneous parametric down-conversion(SPDC) in a nonlinear crystal[6], for it is most accessible and controllable in present technique. One drawback of the photon generated via SPDC is its wide spectrum, which makes its interaction with atoms very difficult. In order to solve this problem, several groups generate a narrow-band photon pair via an optical parametric oscillator(OPO) far below threshold[7, 8, 9, 10, 11, 12]. The property of the two photons produced by this way enable us to directly observe their correlation function by coincident counting, and an interferometer can be used to realize this goal. Goto *et.al.* recently reported the two-photon interference of multimode two-photon pairs with an unbalanced Mach-Zehnder interferometer[10]. The time correlation between the multimode two photons has a multi-peaked structure. In their experiment, the propagation time difference  $T$  between the short and long paths in the interferometer is  $\tau_r/2$ , where  $\tau_r$  is the round-trip time of the OPO cavity. Their results show that the property of the multimode two-photon state induces two-photon interference depending on the delay. In this paper, we report on an observation of quantum interference of multimode two-photon pairs generated via an OPO far below threshold with a Michelson interferometer. In the experiment, we not only discuss the case in which the interferometer is in highly unbalanced, but also consider the case when the interferometer is balanced. In highly unbalanced case, the path propagation difference between the short and long paths is nearly equal to  $\tau_r/3$ . In this situation, only two-photon interference occurs, there is no single photon interference because of quite short coherence length( $<100 \mu\text{m}$ ) measured in our experiment[13]. The time correlation between the multimode two photons still has a multi-peaked structure. We find that the shape of correlation fringe is different from that reported in Ref.[10]. Therefore we conclude that the shape of correlation is dependent on the path difference between two interfering beams. In balanced case, we consider two different situations: one is that the interferometer is perfectly balanced, which means that the path difference is almost zero. In this situation, both two-photon interference and single-photon interference exist simultaneously. The time correlation has multi-peaked structure, but is very different from that in highly unbalanced case. The shape of the fringe is independent on the phase between two interfering beams beside height. We also consider another situation: the interferometer is almost balanced, the path difference is

slightly larger than the coherent length of the single photon. In this situation, there is only two-photon interference. The time correlation observed still has the multi-peaked structure, is similar to that in perfectly balanced situation, and the shape of fringe is also independent on the phase between two interfering beams beside the height. All experimental results are well agreed with the theoretical prediction.

A schematic drawing of the experimental setup is shown in Fig. 1. A cw grating-stabilized external diode laser (Toptical DL100) of wavelength 780 nm is used to generate UV light at 390 nm via a frequency doubler, which consists of a symmetric bow-tie cavity with a 10 mm long type-I phase-matched periodically poled  $\text{KTiOPO}_4$  (PPKTP) inside. The frequency of the laser is precisely locked to Rb atom transition frequency using the saturated absorption technique. The frequency of the doubling cavity is locked to frequency by PDH method[14]. About 50  $\mu\text{W}$  UV light at 390 nm is input to an OPO far below threshold, which consists of a 10 mm long type-I phase-matched PPKTP and a symmetric bow-tie cavity. The triangle cavity C is used to get mode-matched between SHG cavity and OPO cavity. A chopper is used to cut the photons of locking light reflected from the surface of the crystal to avoid possible background noise. The photon generated is multimode photon because of no mode-selected cavity used, and has the comb-like shape of the spectrum[13]. The outputs from OPO are input into a Michelson interferometer. A red filter is used to cut the remaining UV light. The path difference between two interfering beams can be adjusted by moving the mirror M1, which is mounted a piezoelectric transducer (PZT). Both PZT and mirror are fixed on a translation stage. The relative phase between two interfering beams can be actively controlled. The one output of the interferometer is connected to a 50/50 fiber beam splitter (NEWPORT P22s780BB50). Each out port of the fiber BS is connected to an avalanche photon detector (PerkinElmer SPCM-AQR-14-FC). The outputs from detectors are sent to a coincidence circuit for coincidence counting which mainly consists of a picosecond time analyzer (ORTEC, pTA9308) and a computer.

First, we show our experimental result in unbalanced case. In this case, the path difference between two interfering beams  $\Delta L$  is about 170 mm. Before discussing the experimental results, we give the theory about the time correlation function in the unbalanced case which mainly comes from Ref.[10]. The output operator  $a(t)$  of the interferometer can be expressed

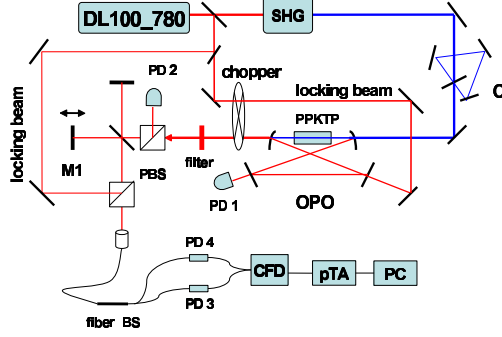


FIG. 1: Schematic of the experimental setup. DL100\_780, diode laser; PBS, polarization beam splitter; PD1 and PD2, photodetectors for locking; PD3 and PD4, avalanche photodetectors; fiber BS, fiber beam splitter; C, triangle cavity; pTA, picosecond time analyzer

by

$$a(t) = \frac{a_{out}(t - T_S) + ia_{vac}(t - T_S)}{2} + \frac{a_{out}(t - T_L) - ia_{vac}(t - T_L)}{2} \quad (1)$$

Here  $T_L$ ,  $T_S$  are the propagation time of the photons along the short and long paths, respectively.  $a_{vac}(t)$  is an annihilation operator of the vacuum entering the interferometer.  $a_{out}(t)$  is the output operator of the OPO which can be defined as

$$a(t) = \frac{1}{\sqrt{2\pi}} \int d\omega a(\omega) e^{-i(\omega_0 + \omega)t} \quad (2)$$

Where  $\omega_0$  is the degenerate frequency of the OPO. The time correlation function is defined as follows

$$\Gamma^{(2)}(\tau) = \langle a^+(t) a^+(t + \tau) a(t + \tau) a(t) \rangle \quad (3)$$

And after dropping the single photon interference terms and considering the probability distribution of timing jitter of detectors, Eq.(3) is expressed as

$$\Gamma_{unbal}^{(2)}(\tau) = C_1 [4\Gamma_{ave}^{(2)}(\tau) \cos^2 \theta + \Gamma_{ave}^{(2)}(\tau - T) + \Gamma_{ave}^{(2)}(\tau + T)] + C_2 \quad (4)$$

with

$$\Gamma_{ave}^{(2)}(\tau) = e^{-\Delta\omega_{opo}|\tau - \tau_0|} \sum_n \left( 1 + \frac{2|\tau - n\tau_r - \tau_0| \ln 2}{T_D} \right) \times \exp \left( -\frac{2|\tau - n\tau_r - \tau_0| \ln 2}{T_D} \right) \quad (5)$$

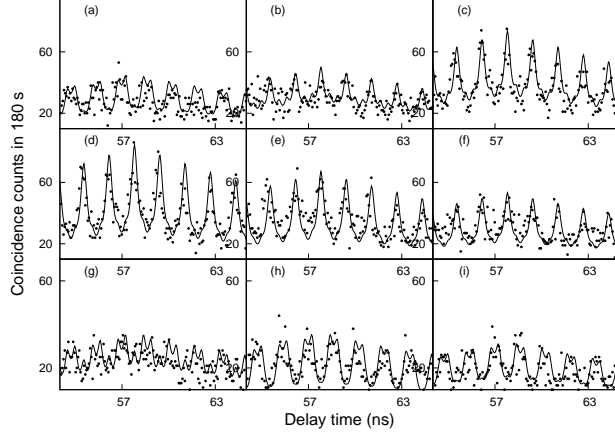


FIG. 2: Experimental results. The phase  $\theta$  increases stepwise by  $\arccos j/4$  from (a) to (i) ( $j=-4, -3, \dots, 4$ ). The dots represent the measured data. The lines are fits by Eq. (4).

Here  $C_1$  is a constant;  $C_2 \propto |\epsilon|^2 \Gamma^{(2)}(0) / \Delta\omega_{opo}^2$ ,  $\epsilon$  is single-pass parametric amplitude gain;  $\Delta\omega_{opo}$  is the bandwidth of the OPO;  $T_D$  is the resolving time of the detectors which is about 220 ps in our experiment;  $\tau_0$  is an electric delay,  $T = T_L - T_S$ . We measure the coincidence counts at  $\cos\theta = j/4$  ( $j = -4, -3, \dots, 4$ ), where  $\theta$  is the phase difference between the two arms of the interferometer. The experimental results are shown in Fig. 2. We set  $\Delta L$  as 170 mm which is about  $\tau_r c/3$  long. The constant parameters are set as follows:  $\tau_0 = 55$  ns,  $\tau_r = 1.63$  ns and  $\Delta\omega/2\pi = 7.8$  MHz. The time correlation has a multi-peaked structure, the shape of the fringe is different from that shown in Ref. [10], this concludes that time correlation is dependent on the path difference. In Fig. 2, the deviation of the points from the fitted lines is probably due to the small  $\tau_r$  which determines the distance between peaks. If  $\tau_r$  is larger, every peak could be more distinguished from each other under the condition of the big resolving time of the detectors, which could achieve better visibility. The fluctuation of phase difference may lead to the deviation as well. Fig. 3 shows the deviation between the locking points of the interference and the fitting points. We find that points (g) and (h) have a little large deviation. This may also come from the fluctuation of phase difference and misalignment of the interferometer, etc.

Next, we discuss the case in which the two interfering beams in the interferometer are almost balanced. According to our measurement on the coherence length of the single photon, which is about 90  $\mu\text{m}$ [13], we divide this case into two different situations: in situation 1, two interfering beams are perfectly balanced, which means there is a single-

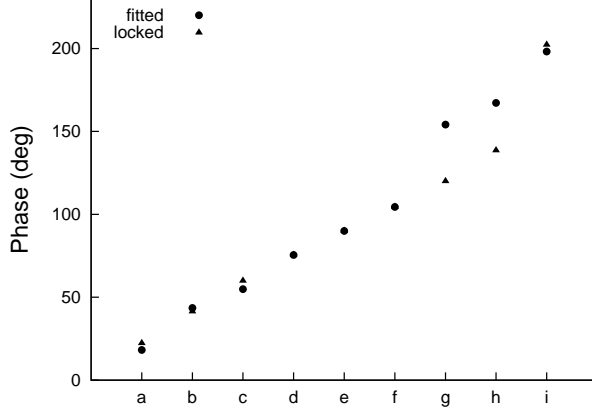


FIG. 3: Phase (fitting) determined by the fitting is plotted against phase (locking) which is the phase locked experimentally. Triangles represent the experimental data and points represent the fitting one. The letter at horizontal axis(a,b,...,i) represents the picture of the same letter in Fig. 2

photon interference besides two-photon interference in the interferometer. In this situation, the time correlation function can be expressed as follow

$$\begin{aligned}
\Gamma_a^{(2)} &= \frac{1}{4} [\Gamma_{ave}^{(2)}(\tau)(1 + \delta) + \delta\Gamma^{(2)}(0)] (\cos \theta + 1)^2 \\
&= \frac{1}{4} [C_1\Gamma_{ave}^{(2)}(\tau) + C_2] (\cos \theta + 1)^2 \\
&\simeq \frac{1}{4}\Gamma_{ave}^{(2)}(\tau)(\cos \theta + 1)^2 \quad (\delta \ll 1)
\end{aligned} \tag{6}$$

In situation 2, two interfering beam are roughly balanced, which means the path difference between two interfering beams is slightly larger than coherence length of the single photon. Therefore, there is no single-photon interference besides two-photon interference. In this situation, the time correlation function is follow

$$\begin{aligned}
\Gamma_b^{(2)} &= \frac{1}{4}\Gamma_{ave}^{(2)}(\cos^2 \theta + \frac{1 + 3\delta}{2}) + \frac{1}{4}\delta\Gamma^{(2)}(0) \\
&= \frac{1}{4}\Gamma_{ave}^{(2)}(\tau)(\cos^2 \theta + C'_1) + C'_2 \\
&\simeq \frac{1}{4}\Gamma_{ave}^{(2)}(\tau)(\frac{1}{2} \cos 2\theta + 1) \quad (\delta \ll 1)
\end{aligned} \tag{7}$$

where  $C_1$ ,  $C_2$ ,  $C'_1$  and  $C'_2$  are constants;  $\delta=4|\epsilon|^2/\Delta\omega_{opo}^2$ . The period of  $\Gamma_b^{(2)}$  is as twice as that of  $\Gamma_a^{(2)}$ .

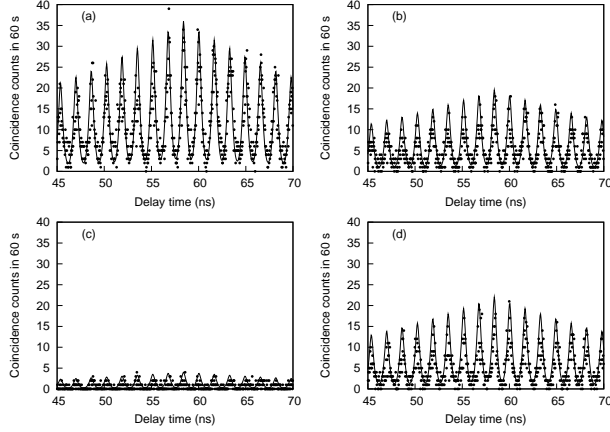


FIG. 4: The time correlation functions of two-photon interference at balanced case are measured at  $\theta=0, \pi/2, \pi$  from (a) to (c). (d) is the function at two-photon interference at an arbitrary phase with  $\Delta L=0.74$  mm for compare.

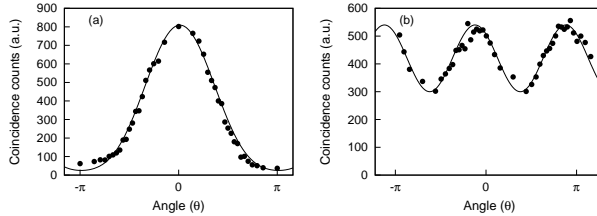


FIG. 5: (a) and (b) are the coincidence counts of two-photon interference in  $\Delta L \approx 0$  and  $\Delta L=0.74$  mm, respectively.

The experiment results are shown in Fig. 4 and Fig. 5. Fig. 4(a)-4(c) indicate the time correlation functions at  $\theta=0, \pi/2$  and  $\pi$  with  $\Delta L \simeq 0$ , respectively. The shapes of three pictures are almost same except the height. The height of the figure in Fig. 4(c) is not exactly zero, because of the phase fluctuation as well as the imperfect 50/50 BS in the interferometer. The experimental results clearly show that time correlation still has the multi-peaked structure, but it is very different from that in unbalanced situation. Fig. 4(d) shows the result when  $\Delta L=0.74$  mm. From the expression of  $\Gamma_b^{(2)}$ , we know the shape of time correlation function is not dependent on phase. We measure it at an arbitrary phase and find it is true. Therefore, we conclude that the shape of the correlation function is independent on the phase and small difference between two interfering beams.

In addition, we measure the coincident counts against the phase between two interfering

beams. Fig. 5(a) and Fig. 5(b) shows the results in situation 1 and 2, respectively. The visibility of the Fig. 5(a) is about 88% against the perfect case of 100% and that of Fig. 5(b) is about 29% against the perfect case of 50%. The possible reason are follow: the shifting of light from ECDL during the experiment; the small shift of mirror positions; the phase fluctuation and so on. Comparing Fig. 5(a) and 5(b), we can see clearly that the period of oscillator in situation 2 is as twice as that in situation 1.

In summary, in this work we observe the quantum interference of multimode two-photon pairs produced by an OPO with an Michelson interferometer which shows a multi-peaked structure. We find that the correlation function is dependent on the path difference and phase between two interfering beams in unbalanced case, which is agree with the Ref. [10]. Furthermore, we find that the time correlation shape in balanced case is independent on the small path difference and phase, beside the height, compared with that in unbalanced case. All experimental results are well agreed with theoretical prediction.

### Acknowledgments

We thank Mr. J. S. Xu and Dr. C. F. Li for their kindly lending of pTA. This work is supported by National Natural Foundation of Science, (Grant No. 10674126), National Fundamental Research Program (Grant No. 2006CB921900), the Innovation fund from CAS, Program for NCET.

- 
- [1] A. K. Ekert, Phys. Rev. Lett. **67**, 661 (1991).
  - [2] C. H. Bennett, G. Brassard, C. Crépeau, R. Jozsa, A. Peres, and W. K. Wootters, Phys. Rev. Lett. **70**, 1895 (1993).
  - [3] K. Mattle, H. Weinfurter, P. G. Kwiat, and A. Zeilinger, Phys. Rev. Lett. **76**, 4656 (1996).
  - [4] D. Bouwmeester, J.-W. Pan, K. Mattle, M. Eibl, and A. Weinfurter, Harald Zeilinger, Nature **390**, 575 (1997).
  - [5] D. Deutsch and R. Jozsa, Proc. R. Soc. London, Ser. A **439**, 553 (1992).
  - [6] D. C. Burnham and D. L. Weinberg, Phys. Rev. Lett. **25**, 84 (1970).
  - [7] Z. Y. Ou and Y. J. Lu, Phys. Rev. Lett. **83**, 2556 (1999).



- [8] H. Goto, Y. Yanagihara, H. Wang, T. Horikiri, and T. Kobayashi, Phys. Rev. A **68**, 015803 (2003).
- [9] M. Scholz, F. Wolfgramm, U. Herzog, and O. Benson, Appl. Phys. Lett. **91**, 191104 (2007).
- [10] H. Goto, H. Wang, T. Horikiri, Y. Yanagihara, and T. Kobayashi, Phys. Rev. A **69**, 035801 (2004).
- [11] C. E. Kuklewicz, F. N. C. Wong, and J. H. Shapiro, Phys. Rev. Lett. **97**, 223601 (pages 4) (2006).
- [12] F.-Y. Wang, B.-S. Shi, and G.-C. Guo, unpublished (????).
- [13] B.-S. Shi, F.-Y. Wang, and G.-C. Guo, unpublished (????).
- [14] R. W. P. Drever, J. L. Hall, F. V. Kowaiski, J. Hough, G. M. Ford, A. J. Munley, and H. Ward, Appl. Phys. B **31**, 97 (1983).